

# OPTIMIZING THE PETRA IV GIRDER BY USING BIO-INSPIRED STRUCTURES

S. Andresen<sup>1</sup>, Alfred-Wegener-Institut Helmholtz-Zentrum für Polar- und Meeresforschung,  
Bremerhaven, Germany

<sup>1</sup>also at Deutsches Elektronen Synchrotron, Hamburg, Germany

## Abstract

The PETRA IV project at DESY (Deutsches Elektronen Synchrotron) aims at building a unique synchrotron light source to provide beams of hard X-rays with unprecedented coherence properties that can be focused to dimensions in the nanometer-regime.

An optimization of the girder structure is necessary to reduce the impact of ambient vibrations on the particle beam. For this purpose, several numerical approaches have been made to simultaneously reach natural frequencies above 50 Hz, a high stiffness and a low mass.

In order to define an optimal girder support, a parametric study was conducted varying both the number and location of support points. Based on the resulting arrangement of support points, topology optimizations were performed to achieve a high stiffness and a high first natural frequency. The following transformation of the results into parametric constructions allowed further parametric studies to find optimal geometry parameters leading to the aimed girder properties. In addition to that, bio-inspired structures based on marine organisms were applied to the girder which likewise resulted in improved girder properties.

## INTRODUCTION

DESY (Deutsches Elektronen Synchrotron) plans to convert the PETRA III (Positron-Elektron-Tandem-Ring-Anlage) storage ring into an ultralow emittance synchrotron radiation source, able to provide beams of hard X-rays with very high coherence properties that can be focused to dimensions in the nanometer-regime and allows the analysis of physical, chemical and biological interactions which occur inside materials between atoms.

In order to receive such highly energetic and low emittance synchrotron radiation, it is fundamental to minimize the impact of ambient vibration on the girders which carry the magnets guiding the particles. An optimization of the girder design is therefore crucial to avoid resonance and

minimize vibration amplitudes.

To achieve the best results, several approaches were followed in a systematic development of new girder designs.

As the definition of boundary conditions has a strong impact on the vibration characteristics and the stiffness, a support study was conducted which varied both the number and location of support points in order to find the optimal support point number and locations. Based on the resulting arrangement of support points, topology optimizations were performed to achieve a high stiffness in combination with a high first natural frequency. The goal of a topology optimization is to find the optimal design of a structure within a specified design space [1]. The applied loads and support conditions, the volume of the structure to be designed and potentially additional design restrictions are known, whereas the size, shape and connectivity of the structure are unknown. The subsequent transformation of the topology optimization result in parametric constructions allowed further parametric studies to determine optimal geometry parameters leading to the aimed girder properties. Furthermore, structures inspired by marine organisms were applied to the girder which also resulted into improved girder properties.

The objective of the conducted studies was to develop girder designs with natural frequencies higher than 52 Hz, a maximal deflection lower than 0.5 mm and a girder mass of maximal 2500 kg.

## SUPPORT STUDY

### Methods

An actual PETRA III girder assembly provided the basis for the study and led to the model layout shown in Fig. 1. The girder was abstracted as a hollow cuboid and meshed with shell elements with an averaged edge size of 0.08 m. The material was characterized by a Young's modulus of  $2.1 \times 10^{11} \text{ N m}^{-2}$ , a density of  $7830 \text{ kg m}^{-3}$  and a Poisson's ratio of 0.3. The defined shell thickness of

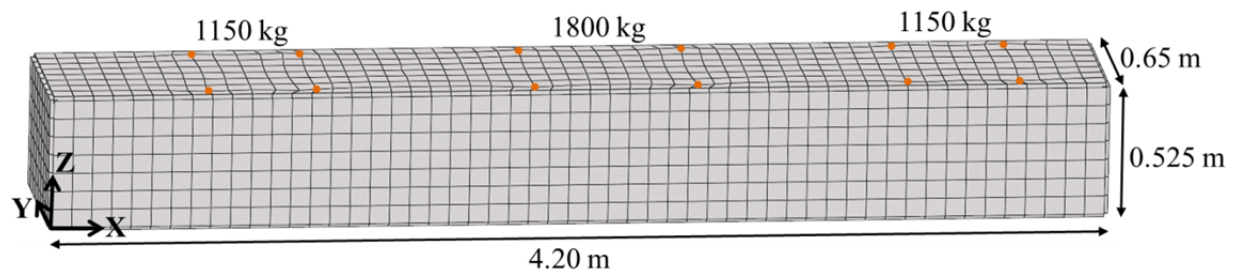


Figure 1: Model assembly considered for the support study. The orange dots show the defined point masses representing the three heavy magnets. The shell thickness of the elements is displayed.

Content from this work may be used under the terms of the CC BY 3.0 licence (© 2018). Any distribution of this work must maintain attribution to the author(s), title of the work, publisher, and DOI.

0.03 m led to a girder mass of 2479 kg. Three heavy magnets were considered each as point masses apportioned among four points.

Table 1 summarizes the analyzed support point configurations. Regarding the study steps 1 and 2, three and four support points, respectively, were defined at the Bessel points of the girder and thus at the lower girder surface. This support point configuration has been considered in previous studies [2]. As to the study steps 3, 4 and 5, the support points were located at the upper girder edges at the specified coordinates. Parameter studies were performed varying the support point locations in the defined range with a step size of 0.1 m. At the specified support points, all translations and rotations were zero.

After the model assembly using the software Rhinoceros, Plug-In Grasshopper, the solver OptiStruct (Altair)

was considered to receive the first natural frequency of the conducted modal analysis.

For each study step, the support point locations leading to the highest first natural frequency were recorded. In addition to that, the girder pedestals were included to estimate their impact on the natural frequency (Fig. 2). Here, an optimal wall thickness of the pedestals in order to reach a high stiffness was considered.

### Results

Figure 3 shows the first natural frequency depending on the support point configuration and the neglect and consideration of the pedestals. Defining the support points at the Bessel points of the lower girder surface led to low first natural frequencies of less than 15 Hz. The first mode shape showed tilts around the support points with highest

Table 1: Configurations of the support study. Depending on the five study steps, the support point (SP) positions were defined and changed along the X axis of the girder.

| Study step | SP   | SP position          | SP start coordinates | SP displacement along X axis Range | Step size | Number of combinations |
|------------|------|----------------------|----------------------|------------------------------------|-----------|------------------------|
| 1          | SP 1 | Lower girder surface | (0.94; 0.325; 0.0)   | -                                  | -         | 1                      |
|            | SP 2 | Lower girder surface | (0.94; 0.325; 0.0)   | -                                  | -         |                        |
|            | SP 3 | Lower girder surface | (3.26; 0.43; 0.0)    | -                                  | -         |                        |
| 2          | SP 1 | Lower girder surface | (0.94; 0.22; 0.0)    | -                                  | -         | 1                      |
|            | SP 2 | Lower girder surface | (0.94; 0.43; 0.0)    | -                                  | -         |                        |
|            | SP 3 | Lower girder surface | (3.26; 0.22; 0.0)    | -                                  | -         |                        |
|            | SP 4 | Lower girder surface | (3.26; 0.43; 0.0)    | -                                  | -         |                        |
| 3          | SP 1 | Upper girder edge    | (0.94; 0.0; 0.525)   | -0.9 - 0.9                         | 0.1       | 6859                   |
|            | SP 2 | Upper girder edge    | (2.1; 0.65; 0.525)   | -0.9 - 0.9                         | 0.1       |                        |
|            | SP 3 | Upper girder edge    | (3.26; 0.0; 0.525)   | -0.9 - 0.9                         | 0.1       |                        |
| 4          | SP 1 | Upper girder edge    | (0.94; 0.0; 0.525)   | -0.9 - 0.9                         | 0.1       | 361                    |
|            | SP 2 | Upper girder edge    | (0.94; 0.65; 0.525)  | -0.9 - 0.9                         | 0.1       |                        |
|            | SP 3 | Upper girder edge    | (3.26; 0.0; 0.525)   | -0.9 - 0.9                         | 0.1       |                        |
|            | SP 4 | Upper girder edge    | (3.26; 0.65; 0.525)  | -0.9 - 0.9                         | 0.1       |                        |
|            | SP 5 | Upper girder edge    | (0.94; 0.0; 0.525)   | -0.9 - 0.5                         | 0.1       |                        |
|            | SP 6 | Upper girder edge    | (0.94; 0.65; 0.525)  | -0.9 - 0.5                         | 0.1       |                        |
| 5          | SP 1 | Upper girder edge    | (2.1; 0.0; 0.525)    | -0.5 - 0.5                         | 0.1       | 2475                   |
|            | SP 2 | Upper girder edge    | (2.1; 0.65; 0.525)   | -0.5 - 0.5                         | 0.1       |                        |
|            | SP 3 | Upper girder edge    | (3.26; 0.0; 0.525)   | -0.5 - 0.5                         | 0.1       |                        |
|            | SP 4 | Upper girder edge    | (3.26; 0.65; 0.525)  | -0.5 - 0.5                         | 0.1       |                        |
|            | SP 5 | Upper girder edge    | (0.94; 0.0; 0.525)   | -0.5 - 0.9                         | 0.1       |                        |
|            | SP 6 | Upper girder edge    | (0.94; 0.65; 0.525)  | -0.5 - 0.9                         | 0.1       |                        |

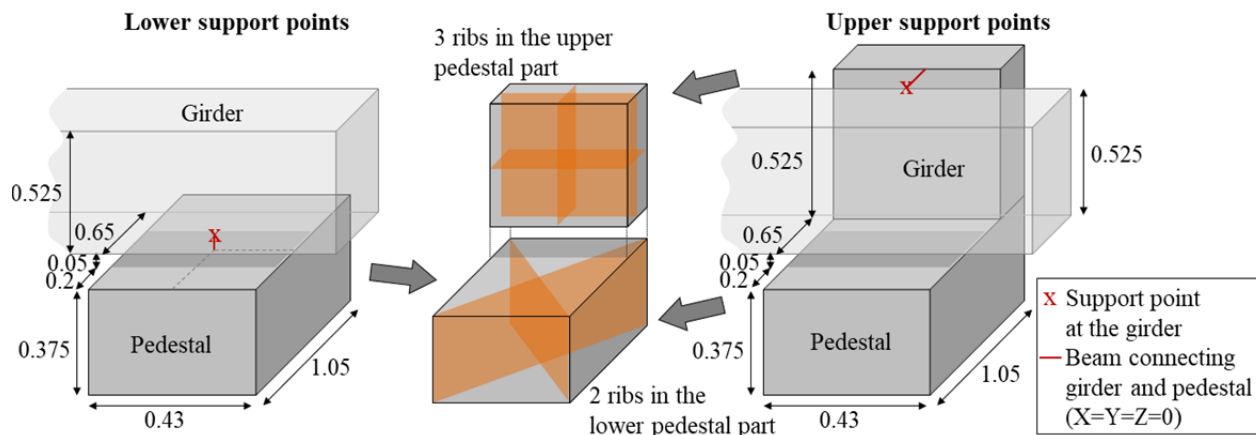


Figure 2: Design of the pedestals. In case of the lower support points, just the lower pedestal part with two ribs was considered, whereas the upper pedestal part with three inner ribs was additionally included for the upper support points.

amplitudes at the locations of the magnets.

Locating the support points at the upper girder edges led to a first mode shape of bending in the Y-Z-plane overlaid with a torsion mode. Here, the highest amplitudes appeared at the lower girder surface far away from the magnets. The first natural frequency increased with the number of support points (Table 2). Considering the pedestals strongly decreases the first natural frequency.

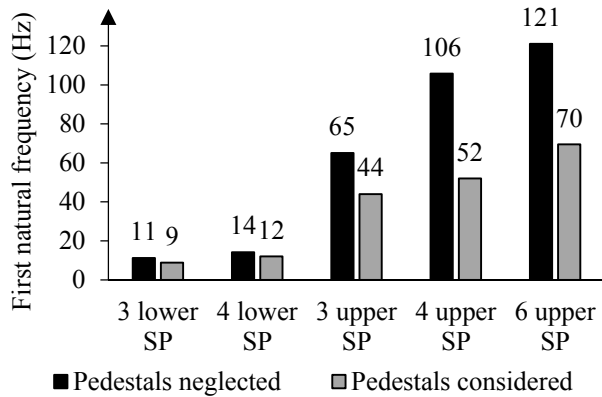


Figure 3: First natural frequency depending on the support point configuration and the neglect and consideration of the pedestals. The frequency is located on top of each bar.

Table 2: Best support point (SP) locations leading to the highest first natural frequency for the three study steps of SP at the upper girder edges.

| Study step | SP   | Best SP location    |
|------------|------|---------------------|
| 3          | SP 1 | (0.44; 0.0; 0.525)  |
|            | SP 2 | (3.0; 0.65; 0.525)  |
|            | SP 3 | (4.16; 0.0; 0.525)  |
| 4          | SP 1 | (0.24; 0.0; 0.525)  |
|            | SP 2 | (0.24; 0.65; 0.525) |
|            | SP 3 | (3.56; 0.0; 0.525)  |
|            | SP 4 | (3.56; 0.65; 0.525) |
| 5          | SP 1 | (0.04; 0.0; 0.525)  |
|            | SP 2 | (0.04; 0.65; 0.525) |
|            | SP 3 | (2.0; 0.0; 0.525)   |
|            | SP 4 | (2.0; 0.65; 0.525)  |
|            | SP 5 | (3.76; 0.0; 0.525)  |
|            | SP 6 | (3.76; 0.65; 0.525) |

### Discussion

Analogous to the result of a conducted support study [3], an increasing number of support points leads to a higher first natural frequency. Moreover, locating the support points close to the magnets has also a positive influence on the vibration characteristics as already mentioned [4].

Considering the pedestals leads to a strong decrease in the first natural frequency. In order to assure a first natural frequency of more than 52 Hz, six support points at the locations listed in Table 2 should be defined. This support configuration was considered in the following studies.

### Simulation

### Structural Statics And Dynamics

## TOPOLOGY OPTIMIZATION

### Methods

The volume shown in Fig. 1 was specified as design space where elements can be removed during the optimization. Besides this, elements around the support points and point masses were manually selected as non-design space. The girder pedestals were neglected. Previous studies have demonstrated that no material in the girder middle is needed to reach a high first natural frequency. Therefore, 30% in the middle of the design space was manually removed to support the generation of clear load paths.

The best support point configuration of six support points gotten from the support study was considered. The material properties were analogous to the support study, while the mesh was made out of solid elements with an average size of 1 cm. A final volume fraction of 0.1 and a first natural frequency of more than 100 Hz were defined as constraints. For this, a modal load case with the point loads shown in Fig 1 was specified considering the first ten natural frequencies. For the second linear static load case, the magnets were abstracted as point loads resulting from the product of the magnet mass and the gravity factor. The topology optimization was conducted using HyperWorks (Altair) and the solver OptiStruct.

With the help of the smoothing function OSSMOOTH and minor manual changes, the resulting structure was 3D meshed. A modal analysis and a linear static analysis were conducted to examine the natural frequencies and the maximal deflection under the load of the three magnets.

Subsequently, curves were derived from the resulting structure and projected onto the outer girder walls using Rhinoceros and the Plug-In Grasshopper as well as algorithms developed in my research section at the Alfred-Wegener-Institut. A shell thickness optimization was conducted to determine the optimal thickness for each rib formed by the curves to meet the requirements stated initially.

### Results

The topology optimization result is shown in Fig 4a. A high virtual element density represents the importance of an element to reach the desired properties. The reanalysis of the resulting structure of 863 kg led to a maximal deflection of 0.03 mm. The first natural frequency is 91 Hz and the connected mode shape showed a local vibration of the lower right bars while the structure close to the magnets revealed low amplitude (Fig. 4b). The shell thickness optimization of the ribs derived from the topology optimization resulted into a variety of structures with properties shown in Fig. 5a. A girder structure with a first natural frequency of 130 Hz, a mass of 1920 kg and a maximal deflection of 0.01 mm is shown in Fig. 5b.

### Discussion

The topology optimization led to a very light structure showing a high first natural frequency and low maximal deflection. Girder structures with even higher natural



Content from this work may be used under the terms of the CC BY 3.0 licence (© 2018). Any distribution of this work must maintain attribution to the author(s), title of the work, publisher, and DOI.

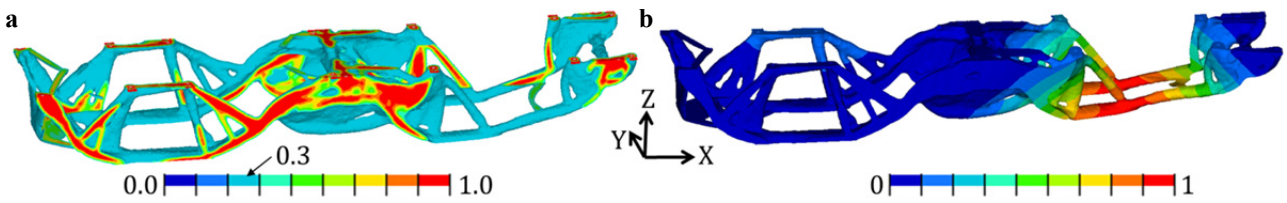


Figure 4: (a) Result of the topology optimization. The coloured scale represents the virtual element density. All elements with a density of at least 0.3 are shown. (b) First mode shape ( $f = 91$  Hz) of the resulting structure of the topology optimization. The coloured scale represents the normalized vibration amplitude.

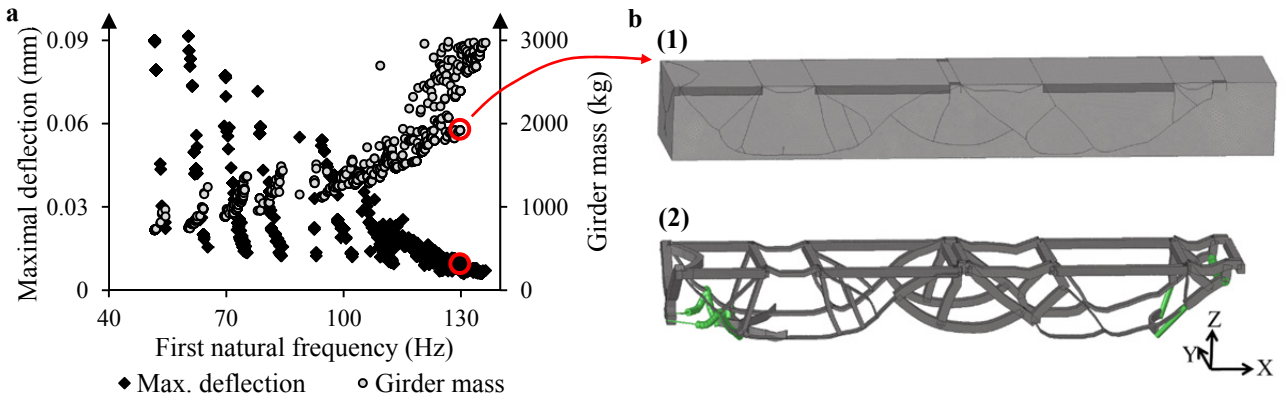


Figure 5: (a) First natural frequency, maximal deflection and girder mass of different girder structures derived from the topology optimization. The girder with the red encircled properties is shown in (b1) entirely and in (b2) with hidden outer walls to visualize the inner ribs and beams derived from the topology optimization (*bright grey*: outer surfaces of the girder, *dark grey*: ribs, *green*: beams).

frequencies can be obtained by integrating ribs and beams derived from the topology optimization results into the girder. As the girder pedestals have been neglected so far, it still has to be demonstrated that including the pedestals, the first natural frequency will remain above 52 Hz.

## BIONIC STRUCTURES

### Methods

Design space, boundary conditions and material properties were specified analogous to the layout of the topology optimization. Thus, the location of the support points and the point masses representing the magnets were fixed, while the girder pedestals were neglected.

The designed lattice structure was based on a point distribution inside the design space. Using the fixed magnet and support points as attractors, the point distribution density was changed locally around the attractors. The lattice was built by connecting each point with a certain number of neighboring points leading to a lattice structure which can be often observed in nature.

In order to reach a high first natural frequency, the outer walls of the design space were also considered. A parameter study was conducted generating 300 structures based on randomly defined parameter values in between the specified definition range of each parameter shown in Table 3. For each structure, a modal analysis and a linear static analysis were conducted.

Table 3: Parameters and their definition range for the lattice structure based on connection of neighboring points and attractors (Attr.).

| Parameters             | Range                               |
|------------------------|-------------------------------------|
| Point distribution:    | Attr. value (m): 0.10 - 0.70        |
|                        | Attr. radius (m): 0.05 - 0.40       |
|                        | Attr. decay factor (m): 1.10 - 2.50 |
|                        | Global value (m): 0.20 - 0.70       |
| Neighbors:             | Number of neighbors: 5 - 25         |
| Outer surfaces:        | Shell thickness (m): 0.01 - 0.05    |
| Lattice cross section: | Outer diameter (m): 0.01 - 0.06     |
|                        | Wall thickness (m): 0.003 - 0.03    |

During the evaluation of the results, structures having a mass of more than 2500 kg and showing a maximal deflection of more than 0.5 mm were neglected. From the remaining structures, the one having the highest first natural frequency was rated as the best lattice structure. Afterwards, the pedestals were considered analogous to the support study to estimate their influence on the natural frequency and the stiffness.

### Results

The inverse values of the maximal deflections (stiffness) and the girder masses were tending to increase with the squared first natural frequency similar to a simple mass oscillator (Fig. 6). However, for a specific stiffness value, structures with different first natural frequencies

were generated, whereby the girder masses remained within permitted values.

Figure 7 shows the best structure considering the pedestals, whose parameter values are summarized in Table 4. The total girder mass was 2489 kg and the maximal deflection 0.02 mm. The first mode shape at a frequency of 70 Hz showed a rotation in the Y-Z-plane with the highest amplitude at the lower girder surface far away from the magnets.

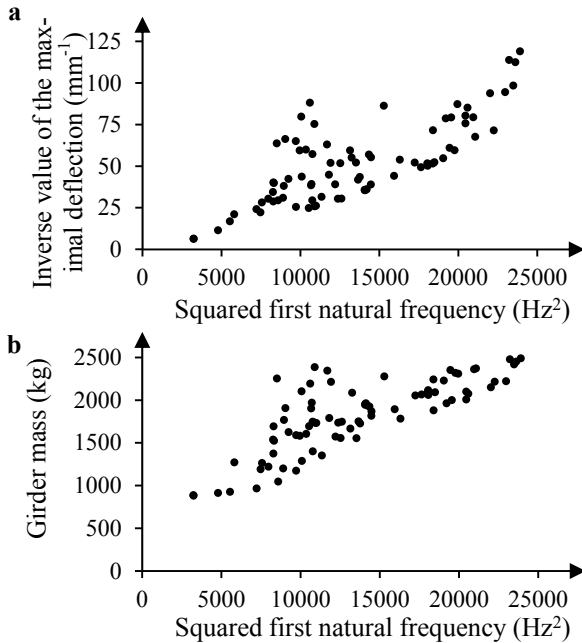


Figure 6: Inverse of the maximal deflection (stiffness) (a) and girder mass (b) depending on the squared first natural frequency for different lattice girder structure.

### Discussion

Using bionic lattice structures in combination with an optimal support point configuration leads to girder assemblies with natural frequencies well above 70 Hz. Moreover, the parametric construction of the lattice structure allows the shift of natural frequencies by leaving the stiffness and mass constant or the other way around. However, production restrictions have not been included yet.

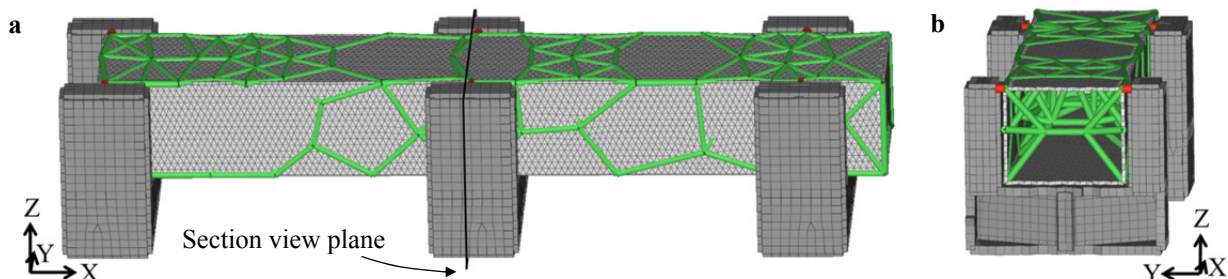


Figure 7: Best bio-inspired lattice girder structure based on connection of neighboring points. (b) shows the section view marked in (a). The shell thickness and beam cross section of the elements are displayed (green: lattice, bright grey: outer surfaces of the girder, dark grey: pedestals, red: beams connecting girder and pedestals).

Table 4: Parameters and their specified values for the best lattice structure based on connection of neighboring points and attractors (Attr.).

| Parameters             |                         | Value |
|------------------------|-------------------------|-------|
| Point distribution:    | Attr. value (m):        | 0.27  |
|                        | Attr. radius (m):       | 0.17  |
|                        | Attr. decay factor (m): | 2.47  |
|                        | Global value (m):       | 0.41  |
| Neighbors:             | Number of neighbors:    | 6     |
| Outer surfaces:        | Shell thickness (m):    | 0.02  |
| Lattice cross section: | Outer diameter (m):     | 0.04  |
|                        | Wall thickness (m):     | 0.014 |

### CONCLUSION

The study shows the high potential of structural optimization for passive vibration control. A variation of the girder structure allows a natural frequency shift keeping the stiffness and the mass constant.

Innovative, bio-inspired girder structures were generated with improved properties regarding stiffness, natural frequencies and lightweight design.

### ACKNOWLEDGMENTS

I would like to thank my colleagues from Alfred-Wegener-Institut for providing the algorithms to generate the bionic lattice structures and my colleagues from DESY for the collaboration and the frequent comments on my work.

### REFERENCES

- [1] M. P. Bendsøe and O. Sigmund, “*Topology Optimization, Theory, Methods and Applications*”, 2<sup>nd</sup> Edition, Springer-Verlag Berlin Heidelberg, Germany, 2004.
- [2] S. Andresen “Untersuchung von Eigenschwingung und Leichtbaupotenzial unterschiedlicher Gitterstrukturen am Beispiel von Magnetuntergestellen von Teilchenbeschleunigern”, presented at NAFEMS DACH, Bamberg, Germany, May 2018, unpublished.
- [3] X. Wang, Z. Yan, H. Du and L. Yin, “Investigation of mechanical stability for SSRF girder”, in *Proc. MEDSI’04*, 2004, Grenoble, France.
- [4] D. Mangra, S. Sharma and C. Doose, “Performance of the vibration damping pads in the APS storage ring”, in *Proc. MEDSI’00*, 2000, Wurenlingen/Villigen, Switzerland.